Local-bonding trends in the cohesion of metals

Gayle S. Painter and F. W. Averill*
Metals and Ceramics Division, Oak Ridge National Laboratory, P.O. Box 2008, Oak Ridge, Tennessee 37831-6114
(Received 24 February 1994)

First-principles atomic-cluster calculations have been carried out in the local-density approximation (LDA) for small clusters (six-atom octahedra) for each metallic element of the Periodic Table through Cu. Trends in ground-state properties of these clusters have been found to bear a significant relationship to corresponding trends in the crystalline solids. Binding energies and bond lengths for these clusters, which form fragments of the crystal lattice, display trends with atomic number which are very similar to the trends in experimental cohesive energies and lattice constants for the solid. An even closer correspondence is found when comparing with results from LDA band-structure calculations. The accuracy of small clusters in representing these trends in solids indicates that local interactions are dominant in determining the variations in cohesive and structural properties that distinguish one metal from another. Energy shifts that result from coupling the cluster to the rest of the solid are rather unform within different families of metals.

I. INTRODUCTION

The study of atomic clusters has experienced rapid growth over the last decade, stimulated by laser vaporization and other experimental procedures and the development of accurate theoretical techniques.[1,2] Clusters are often described as forming a new state of matter for many materials in that they exist in a phase different from that usually found in nature. Generally, the term "cluster" is applied to a molecular form of a material which is normally a solid. Clusters thus display properties that are intermediate between the atomic and bulk limits. It is of interest from both a fundamental as well as an applied point of view to know how the properties of small clusters evolve with size (number of atoms) and how this evolution depends on atomic number. Metallic clusters are of particular interest in part due to the discovery of shell filling (magic numbers) in alkali clusters.[3] They also exhibit electronic properties which are strongly dependent on cluster size distribution, and consequently they have useful applications. A number of experimental[4-6] and theoretical[7-14] studies have been conducted in order to determine the size dependence of cluster properties. Results show that the number of atoms required to reach the "bulk limit" depends on the specific property in question and the relative importance of localization. For example, interatomic separations show rapid convergence to the bulk limit,[4,7,10] but response properties[5,6] that depend on the densities of states converge slowly with the number of atoms. Also, binding energies of atomic clusters depend upon cluster morphology to a moderate extent, and converge to the bulk limit at a slow rate.[9-14] In most studies of convergence behavior of cluster properties with regard to the number of atoms, clusters of a single material are normally considered, and absolute convergence in a specific property is examined. A different perspective is taken in this work where cluster/bulk property relations are examined across a series of elements to identify how clusters of fixed symmetry and number of atoms represent *trends* with atomic number in the corresponding set of solids. The motivation here is simple—the interactions between different components of a system are often determined by how their properties compare on a *relative* basis, rather than one which is absolute, e.g., chemical behavior in terms of electronegativities. In the case of metal clusters, for example, it is of interest to know how the intrinsic strengths of clusters of different metals compare relative to one another and how this trend compares with the trend in bulk cohesive strengths. A close correlation between property trends is indicative of a commonality in the bonding interactions underlying the relevant properties in clusters and solids. In addition to improving our understanding about the evolution of bulk properties from those of small clusters, knowledge of the relation between bulk and cluster property trends provides insight into the metal-metal bonding characteristics that distinguish one metal from another.

Results from a study based on calculations of cluster property trends in the first transition-metal series have been reported earlier.[15] Binding energies of six-atom clusters were found to display a trend with atomic number which accurately represents the trend in cohesive energies of the corresponding transition-metal crystalline phases. In the present work, we examine trends in binding energies and interatomic separations for all metallic elements from hydrogen through copper. We find that very small clusters (six atoms in O_h symmetry) display incipient bulk properties showing trends that mirror those found in the limit of the solid. Characteristics emerge in the trends that distinguish three families by bond type (simple, *sp*-bonded II A, and the transition metals). Within each family, the cluster trend represents the crystalline trend very well. If the size dependence is carried to the extreme of the diatomic cluster, the trend in cohesive energies remains quite recognizable for the transition-metal series (although with reduced accuracy relative to the O_h cluster trend). However, the diatomics do not maintain the trend very well for the *sp*-bonded

II A metals, and the case of H is distinctly different and no longer fits the alkali trend found with octahedral clusters. Detailed results will be presented in Sec. III of this paper, and the implications of these findings on our understanding of the metallic bond will be discussed in Sec. IV.

II. METHOD

The principal objective in this study was to determine how trends in binding energies and interatomic separations calculated for small cluster fragments of crystalline metals relate to trends with atomic number of the solids. A number of factors can affect these trends, but in this work we wish to isolate effects to the principal one of chemical bonding. To this end, calculations were carried out for clusters in O_h symmetry, keeping the number of atoms fixed, changing only atomic type as we progress from hydrogen to copper. Bond lengths were determined by minimization of the total energy within the constraint of O_h symmetry.

The choice of octahedral O_h symmetry defines a fragment of the fcc lattice, corresponding to most of the crystal symmetries in this set of elements. With some distortion the octahedron is also a fragment of the bcc and hcp lattices, covering the remaining elements in this study. Only results for the regular octahedral symmetry are reported here, however, since energy changes with the descent in symmetry are secondary to the principal energy factors considered in this work. The choice of such small clusters as treated here emphasizes the dependence of trends on atomic number in the regime where cluster properties exhibit rapid evolution with size.

Calculations were carried out in the local-density approximation[16,17] (LDA) using the exchange-correlation functional of Vosko, Wilk, and Nusair.[18] The first-principles augmented Gaussian-orbital-cluster method[19] was used to calculate the self-consistent electronic structure, total energy, equilibrium internuclear separations, and gradient forces on the atoms. This linear variational technique is a full-potential approach, and with the use of an extended basis of Gaussian tail functions, the only significant source of inaccuracy is the LDA itself. Basis sets of double-zeta quality were generated using Gaussian exponent parameters from published data. Parameters for the transition-metal atom Gaussian basis sets were taken from Wachters'[20] [14s,10p,6d] set for the first-row transition metals and optimized in atomic LDA calculations, using supplementary functions and the procedure of Hay[21] for 3d orbitals. Gaussians for H and Li-row atoms were taken from van Duijneveldt[22] and similarly solving the atomic wave equations to optimize the atomic orbitals within the LDA. For each metallic element (from H through Cu), the cluster was relaxed according to the calculated gradient force on the atoms, determining the ground-state total energy and metal-metal bond length.

III. RESULTS

Metallic elements in the series H through Cu display a wide range of mechanical properties.[23] These cover extremes such as the softness of K, with its low cohesive strength (less than 1 eV/atom binding energy) and large unit cell (Wigner-Seitz radius, $R_{WS}=4.7$ bohr), to the hardness and high cohesive strength (greater than 5 eV/atom binding energy) in the transition metals Fe, Co, and Ni, which bond with small interatomic separations ($R_{WS}<2.7$ a.u.). The calculated binding-energy curves for the clusters that make up this study clearly show characteristics in qualitative agreement with the magnitudes of corresponding bulk mechanical properties, such as elasticity.

Atomic-cluster binding-energy curves for a group of metals, which display a diversity of bonding characteristics, are shown in Fig. 1. The binding energy is evaluated by calculating the total energy of each cluster and subtracting the sum of atomic total energies, also calculated in the LDA. The parameter D measures the displacement of the atoms from the center of the cluster (see inset, Fig. 1). For compressed bond lengths, the binding energy is small and the force on each atom (negative slope of the energy curve) is directed out from the cluster center (repulsion among atoms of the cluster). As the cluster expands and relaxes, the binding increases until the restoring forces vanish (at the ground state). For larger values of D the expanded cluster binding becomes weaker, and the restoring force on each atom is directed inward and anharmonic components grow. The size of this restoring force and the way it depends upon D characterizes the elastic properties of the cluster in much the same way lattice stiffness is probed by atom displacements in a crystal.

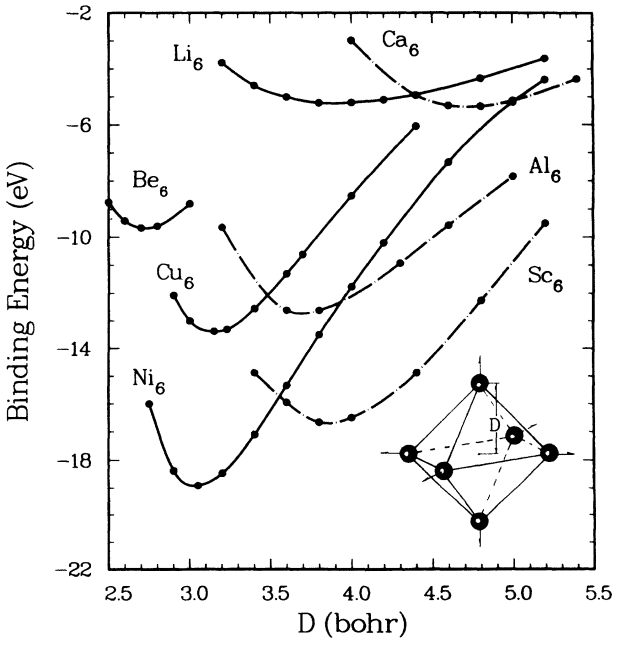

FIG. 1. Binding-energy curves for regular octahedral clusters of various exemplary metallic elements from Li through Cu. The binding energy (cluster energy minus sum of atom energies) is plotted as a function of cluster dimension $D=b/\sqrt{2}$ where b is the metal-metal bond length (see inset).

The binding-energy curves thus determine the equilibrium bond lengths by the energy minimum and reflect the elastic properties through the restoring force behavior. The equilibrium size of each of the clusters in Fig. 1 appears qualitatively consistent with each corresponding observed bulk-crystal unit-cell size. For example, there is a great contrast between the large Ca_6 cluster and the small Be_6 cluster (a volume ratio of five), just as there is with the unit cells of the crystalline counterparts. This qualitative correspondence is also apparent in the elastic properties, as indicated by the slopes and curvatures of the cluster binding-energy curves. For example, of the clusters shown in Fig. 1, the softness of Li and Ca contrasts strongly with the hardness of Ni, and the cohesive strengths of Be, Al, Sc, and Cu are all intermediate with respect to these extreme cases. At this qualitative level then, small fragments of the crystalline solid display elastic properties that are physically significant compared with those of the bulk. As found for the first transition-metal series,[15] incipient bulk cohesive properties are quite recognizable in small elemental clusters in a way that correctly distinguishes one metal from another.

A measure of how well the clusters describe *trends* in bulk cohesive properties is provided by the variations in cluster binding energies compared with variations in cohesive energies of the bulk as the atomic number changes. If the *difference* between energy values for corresponding elements of the bulk and cluster systems is slowly varying through the series, relative energies among elements in the bulk will be accurately represented in the cluster results. Similar trends will then be observed in cluster and bulk cohesion, even though absolute differences between the two may be large.

In Fig. 2 calculated binding energies of the clusters for elements Be through Cu are compared with *experimental* cohesive energies for the crystalline solids. The transition-metal results are the same as reported in Ref. 15. The group-IIIB metal Al is graphed next to the nearest metallic element treated here, which is Cu (group IB), and the slight difference in binding energy between Cu to Al is calculated to be nearly the same for the crystal and the cluster. Indeed, the trend in experimental

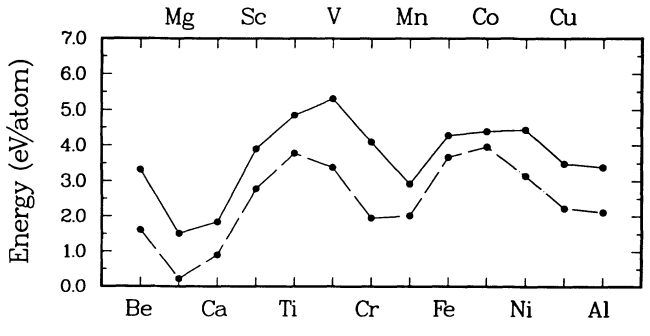

FIG. 2. Octahedral-cluster binding energies compared with experimental bulk cohesive energies for *sp*-bonded metals and 3*d* transition metals. Solid lines connect experimental energies and dashed-dotted lines connect calculated binding energies.

bulk cohesive energies is rather well represented by the small cluster model across the entire series of metals considered here (alkali metals are discussed separately below). The most noticeable deviations from the experimental trend are observed in the Ti–Mn sequence and around Co. However, the origin of this discrepancy in the trend is explained by the occurrence of identical deviations in results calculated for the crystalline solid by LDA band-structure methods. These features must, therefore, originate in the LDA itself (and in particular, in the *atom* reference) rather than reflecting a cluster-size effect.

The absolute difference in cohesive energies between the cluster and crystalline phase for a specific element is large,[24] reaching almost 2.0 eV/atom at V. For discussion of trends, however, it is not the absolute but the *relative* differences that are important, and these have been shown to be small in the 3*d* transition metals.[15] In Fig. 2 we see that the cluster binding energies are all smaller than corresponding experimental cohesive energies for the solid. Since cohesive energies from band-structure calculations all show *overbinding* typical of the LDA, the cluster binding energies must cross the experimental curve in converging to bulk LDA results as the number of atoms increases. So the situation of clusters showing closer agreement with experiment than found in energy-band calculations (for Mn, Fe, and Co in Fig. 2) is simply fortuitous.

The influence of the LDA on features of the cohesive-energy trend can be distinguished from intrinsic cluster-bonding effects by comparing binding energies with crystal cohesive energies[26] from the LDA energy-band calculations of Morruzi, Janak, and Williams[27] (MJW). Their results, obtained for either fcc or bcc crystal structures, are graphed in Fig. 3(a), along with octahedral- and diatomic-cluster binding energies calculated in this work (spin-polarization effects included). Essentially all qualitative features in the variation in cohesive energy through the series of bulk metals are represented by corresponding structure in the graph of octahedral-cluster binding energies. Quantitatively the cluster-binding energies are all smaller than the LDA energy-band cohesive energies, but in spite of the truncation of convergence in cluster size, cohesive-energy differences for one metal relative to another are very accurately described by the octahedral clusters. Spin-polarization effects on the cluster binding energies are small on the scale of Fig. 3(a) (less than 0.10 eV/atom), with the exception of Mn, Fe, and Co (where polarization has increased the binding by 0.15, 0.69, and 0.56 eV/atom, respectively). These effects closely parallel spin-polarization cohesive stabilization in band-structure calculations, so that the cluster trend displayed in Fig. 3(a) properly reflects that of the solid.

The diatomic-cluster results included for comparison in Fig. 3(a) further emphasize the rapid emergence of trends in the cohesion of solids, particularly in the transition metals. Certainly the occurrence of the largest cohesive strengths of Ti and V in the first part of the series and Fe and Co at the end of the series is reflected in the strong bonding found in the diatomics. But while the general double-peaked shape observed in the transition-

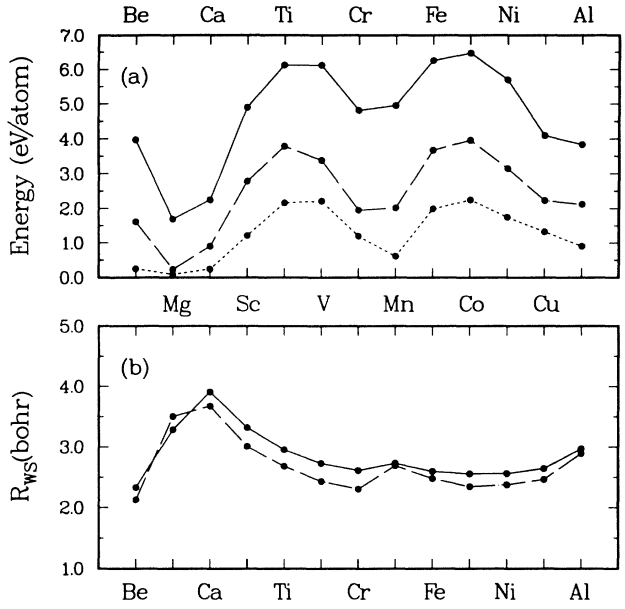

FIG. 3. A comparison of (a) crystalline and cluster binding energies and (b) crystal and cluster Wigner-Seitz radii R_{WS} calculated within the LDA for *sp*-bonded group-IIA metals and the first transition-metal series. The bulk results are from band-structure calculations (Ref. 27) and the cluster results are computed in this work. Solid lines connect results for the solid and corresponding octahedral-cluster values are connected by dashed-dotted lines. Values for diatomic clusters are connected by dashed lines.

metal cohesion curve is present at the diatomic level, details of structure are not as well represented as they are by the octahedral clusters. These structural features (e.g., the Cr to Mn variation resulting from the weak diatomic Mn-Mn bond[28]) evidently reflect the role of *multicenter* bonding, absent in the diatomic but present in the octahedron. This is especially the case with the group-IIA elements, which bind very weakly as diatomics. The diatomic clusters do not represent the bulk trend nearly as well as the octahedral clusters for this family of metals.

It is clear from Fig. 3(a) that octahedral clusters represent the trend in bulk cohesive energies very well across the whole series of elements studied here. Closer examination shows that there are smaller scale *changes* in the magnitude of cluster-bulk energy separation that correlate with the bonding type, defining three families (alkali metals, *sp*-bonded IIA metals, and 3*d*-bonded transition metals). The family of *sp*-bonded group-IIA metals show octahedral-cluster binding energies lying uniformly about 1.5 eV/atom below the bulk cohesive energies, except for Be which deviates in showing a 2.4-eV/atom difference.[29] Even though the cluster-bulk energy difference is greater for Be than for the other IIA clusters, the *structure* in the binding-energy trend [Be-Mg-Ca in Fig. 3(a)] is still consistent with that of the solid.

Within the transition-metal series from Sc through Cu, the cluster results reproduce the bulk LDA cohesive-energy trend especially well. The regularity in cluster-bulk trends suggests that bond localization is most important in this series. For Sc through Cu, LDA bulk cohesive energies[27] vary between 4.1 and 6.5 eV/atom; the difference between bulk and cluster energies in Fig. 3(a) ranges from 1.86 to 2.93 eV/atom (Cu and Mn, respectively). The differences between cluster and bulk energies deviate from a constant by less than 1.1 eV/atom in the 3*d* series. Separating the case of Cu, with its closed 3*d* shell from the rest of the (open 3*d* shell) transition metals reduces the maximum deviation in cluster-bulk energy differences to less than 0.8 eV/atom. But the spread in intrinsic LDA errors for this series of bulk metals[27] is about 1.1 eV/atom, so deviations from the trend do not exceed the relative errors of the LDA itself in this series. The octahedral clusters show a 96% linear correlation[31] with the bulk cohesive energies, compared with a 90% correlation for the diatomics.

The role of LDA error and its appearance in both cluster and bulk calculations can be observed by comparing the cluster binding-energy trend with the experimental bulk cohesive energies in Fig. 2. There, breaks in the trend of cluster binding energies, as compared with experiment, were found to occur as we progress from Ti to V, Cr to Mn, and Co to Ni. But these breaks also occur in the energy-band trends, as can be seen in Fig. 3(a). Their common occurrence in these different models identifies the source of these particular features as the LDA itself. The representation of such structural details in the bulk trend by the octahedral cluster is rather remarkable. Nearly *all* details of structure in the crystal LDA binding-energy plot of Fig. 3(a) appear well represented by the cluster results. This is very suggestive that *structure* in the cohesive-energy trend for this series of solids originates primarily from the localized bonding present within the primitive cluster itself. The effect on cohesion of coupling the cluster to the rest of the solid is a cluster-to-bulk cohesive-energy shift that is rather *uniform* from element to element.

Interatomic separations corresponding to lattice constants and molecular bond lengths are known to be more accurately calculated than total energies in the LDA. Bond lengths are also more rapidly convergent with cluster size than binding energies. Using the equilibrium cluster bond lengths and treating the octahedral cluster as a fragment of the crystal, it is possible to compare with Wigner-Seitz radii from LDA band-structure calculations.[27] For the fcc crystals (the symmetry adopted by MJW for all elements of Fig. 3 except V, Cr, and Fe), the Wigner-Seitz radius is related to the cluster dimensional parameter D, by $R_{WS}=2D/(16\pi/3)^{1/3}$. For the bcc crystals (H, the alkalis, V, Cr, and Fe in MJW), $R_{WS}=\sqrt{2}D/(8\pi/3)^{1/3}$ (regular octahedral symmetry was retained for the cluster without the tetragonal distortion characteristic of the octahedral fragment of the bcc lattice).

Band structure and cluster evaluations of R_{WS} are compared in Fig. 3(b). The trend in interatomic separations in the crystal is quite well represented by the cluster. As typically found for small lattice fragment clusters, bond lengths are about 10% contracted relative to the bulk parameters, reflecting the dominance of near-neighbor interactions in determining lattice constants.

Spin polarization affects the cluster properties in much the same way as observed in the band-structure calculations. Compared with non-spin-polarized ground-state properties, clusters show a magnetic expansion paralleling the phenomenon in the crystal.[27,32] The effects of spin polarization on cluster interatomic separations range from negligible, (less than 0.01 bohr change) for most elements, to slight (0.05 bohr for Co) to significant (0.22 bohr for Fe and 0.55 bohr for Mn). The magnetic-order-induced volume expansion[32] (magnetic expansion) of Mn appears in both cluster and solid trends as the break in R_{WS} at Mn. Its enhancement in the cluster is a consequence of the larger spin moment in the cluster compared with the solid[33] and the greater relaxation freedom for expansion in the cluster. Non-spin-polarized calculations give R_{WS} values for Fe and Mn falling on a smooth curve extrapolated from Cr to Co [Fig. 3(b)].

Turning to other elements, the case of Mg deserves comment in that while the R_{WS} value for the Mg_6 cluster is within the stated range of convergence to the bulk (10%), it differs from all the other clusters in showing an interatomic bond length which is *larger* than the bulk value [Fig. 3(b)]. The origin of this feature is the symmetry constraint on the cluster. In geometry-optimized LDA cluster calculations[34] for Mg clusters, the six-atom cluster takes a rectangular bipyramidal ground-state geometry with a binding energy that is larger by 0.30 eV/atom[14,34] relative to our result. The square bipyramidal geometry, more closely related to our regular octahedron, is found to lie 0.25 eV above this ground-state geometry[34] (within 0.05 eV/atom of the result obtained here) with an average of bond lengths of 6.58 bohr. This is in close agreement with our calculated equilibrium bond length of 6.39 bohr, which yields the R_{WS} value in Fig. 3(b). Thus, it appears that this expansion of the cluster bonds compared with the interatomic separations for crystalline Mg is a result of weak binding in the constrained regular octahedron for Mg_6.

The remaining family of metals that make up this study is the alkali group (plus hydrogen), and calculated cluster binding energies are compared with band-structure cohesive energies[27] in Fig. 4(a). The trend in bulk cohesive energies is rather well represented in the octahedral-cluster trend, with the two graphs maintaining an energy separation near 0.5 eV/atom, and Li deviating from the trend by about 0.3 eV/atom. The diatomic trend [dashed curve, Fig. 4(a)] represents only the relative order of binding energies from Li to K and deviates entirely at H. Hydrogen forms a very stable diatomic molecule with much greater binding energy (4.75 eV dissociation energy[35]) than the fcc solid treated by MJW (1.3 eV/atom) and the cluster results accurately reflect this behavior. While the diatomic represents only the H_2 molecule, the multicenter bonding in H_6 has begun to mimic the metallic bond of solid H.

The trend in Wigner-Seitz radii of the alkali metals is given very well by the octahedral-cluster trend [Fig. 4(b)]. The changes in slope at Li and Na in progressing through the bulk series, although subtle, are accurately mirrored in the cluster trend as well. This again reflects the high accuracy of the small cluster in representing lattice-

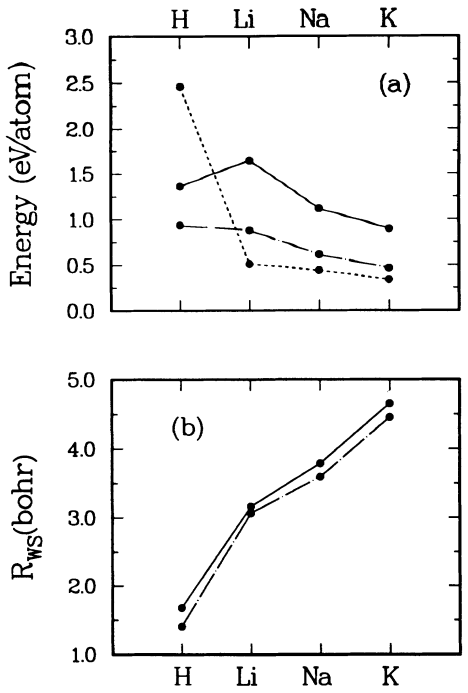

FIG. 4. A comparison of trends in (a) cluster binding energies and (b) Wigner-Seitz radii R_{WS} for H and the first three alkali metals. Solid lines denote calculated bulk results of Ref. 27 and dashed-dotted lines connect octahedral-cluster values. Diatomic results are connected by dashed lines.

constant trends in crystalline metals. As a class, the alkali clusters show the smallest absolute separations in binding energy relative to the bulk (all less than 0.8 eV/atom) compared with cluster-bulk energy differences of up to 2.9 eV/atom in the transition-metal series. Yet the energy differences *average* over members of the family to about 45% of the limiting bulk cohesive energy values in *both* families. This may appear counterintuitive with our concept of bond localization in the transition-metal series, dominated by $3d$ bonding, compared with the more delocalized $s(p)$ bonding in the alkalis. But greater bond localization means greater bond strength and associated cohesive energy contribution, relative to the more delocalized sp bonds. This is clearly displayed in energy-band calculations of the sp and d contributions to the hydrostatic pressure in metals.[36] The $3d$ contribution to the cohesion in transition metals dominates the sp contribution, so that incomplete coordination in the lattice fragment cluster will be accompanied by a larger separation between cluster binding energies and bulk cohesive energies for transition metals compared with the alkalis.

It is interesting that the group-IIA clusters, composed of closed-shell atoms, are characterized by binding energies that do not deviate significantly from the trend in bulk cohesive energies in Fig. 3(a). The success of the LDA in describing the mechanism underlying the van der Waals interaction,[37] although not complete, is reflected in these results. It is also interesting that the cluster result of 0.23 eV/atom binding in Mg_6 compares closely with calculations[38] of the pair-potential binding-energy contri-

bution of only 0.25 eV/atom, indicating the necessity of volume-dependent (delocalized) energy contributions to reach the cohesive energy of 1.7 eV/atom for crystalline Mg.

IV. DISCUSSION

In this study we have found that small lattice-fragment atomic clusters accurately represent trends in cohesive energy and interatomic separations of the corresponding bulk-crystal phases of metallic elements in the series from H through Cu. Density-of-states (electron delocalization) effects are required to achieve convergence to the bulk limit in an absolute sense, but the *relative* values of observables such as cohesive energies and lattice constants are reliably determined by the local bonding factors present in a six-atom octahedral cluster. This characteristic, previously reported for the first transition-metal series,[15] extends with good accuracy to the group-IIA and alkali metals as well and can be considered quite generally valid. This correspondence of trends means that *variations* in these properties with atomic number are a result of local-bonding interactions. Thus, *relative* effects in a series of elements can be deduced with far fewer atoms than usually required for absolute convergence of a particular property of a given cluster. This is especially important with regard to energetics, since these phenomena usually involve energy *differences* rather than absolute values.

Given that *all* of the atoms of the octahedral cluster are actually surface atoms, how does such a small fragment of the solid describe trends as well as it does? The electron density in the volume between atoms is fundamental to most descriptions of bonding, and the density is the central element of density-functional theory. The electronic density at the unit-cell boundary was found to be a controlling factor in the success of the ideal-metal theory.[39] In our cluster calculations, the electron density in the interstitial volume (thus corresponding to a cell-boundary region of the solid) is found to be very nearly the same as calculated by band-structure methods. The rapid convergence of the density in this region, coupled with its importance in the metallic bond, is one of the key factors in the accuracy of the cluster trends.

The picture of metallic bonding suggested by these results is one in which local interactions determine the *variations* in cohesive strength with atomic number. The effect of coupling the cluster to its environment is to produce delocalization shifts in binding energies and bond lengths to bulk limiting values by amounts that are nearly uniform (within each family). We note that this view is consistent with findings from theories that inherently include delocalization effects, such as the ideal metal model.[39] There cohesive energies are generally in the correct range (i.e., the aforementioned shift anticipated from coupling the cluster to the rest of the solid is well accounted for), but structure in the cohesive-energy trend can be weak (when the local-bonding details are important). The cluster model and the ideal-metal theory are in a sense complementary in their treatment of short-range and long-range aspects of the metallic bond, respectively.

Aside from the understanding of the metallic bonding and the origin of trends in cohesion which these results provide, other uses are suggested. In the development of "embedding" schemes, the importance and role of locality are identified, and the coupling effects between cluster and the rest of the solid are better defined. These findings are also directly related to the development of methods for determining crystal binding energies from atomic-cluster calculations.[40] In connection with the synthesis of new materials, the direct correspondence between cluster and bulk trends suggests that known bulk cohesive properties may serve as a basis in strategies for the design of new cluster-assembled materials.[41]

ACKNOWLEDGMENTS

This work was supported by the Division of Materials Science, Office of Basic Energy Sciences, U.S. Department of Energy under Contract No. DE-AC05-84-OR21400 with Martin Marietta Energy Systems, Inc. The authors thank F. W. Kutzler and M. H. Yoo for helpful comments on the manuscript.

*Permanent address: Judson College, Elgin, IL 60123.

[1] *Cluster Models for Surface and Bulk Phenomena, NATO Advanced Study Institute, Series B: Physics,* edited by G. Pacchioni, P. S. Bagus, and P. Parmiagiani (Plenum, New York, 1992).

[2] *Clusters and Cluster-Assembled Materials,* edited by R. S. Averback, J. Bernholc, and D. L. Nelson, MRS Symposia Proceedings No. 206 (Material Research Society, Pittsburgh, 1991).

[3] W. A. deHeer, W. D. Knight, M. Y. Chou, and M. L. Cohen, in *Solid State Physics,* edited by H. Ehrenreich, F. Seitz, and D. Turnbull (Academic, New York, 1987), Vol. 40, p. 94.

[4] P. A. Montano, G. K. Shenoy, E. E. Alp, W. Schulze, and J. Urban, Phys. Rev. Lett. **56**, 2076 (1986).

[5] K. E. Schriver, J. L. Perrson, E. C. Honea, and R. L. Whetten, Phys. Rev. Lett. **64**, 2539 (1990).

[6] K. Rademann, O. Dimopoulou-Rademann, M. Schlauf, U. Even, and F. Hensel, Phys. Rev. Lett. **69**, 3208 (1992).

[7] B. K. Rao, S. N. Khanna, and P. Jena, Phys. Rev. B **36**, 953 (1987).

[8] E. Engel and J. P. Perdew, Phys. Rev. B **43**, 1331 (1991).

[9] B. Delley, D. E. Ellis, A. J. Freeman, E. J. Baerends, and D. E. Post, Phys. Rev. B **27**, 2132 (1983).

[10] B. K. Rao and P. Jena, J. Phys. F Met. Phys. **16**, 461 (1986).

[11] K. Raghaven, M. S .Stave, and A. E. DePristo, J. Chem. Phys. **91**, 1904 (1989).

[12] J. D. Kress, M. S. Stave, and A. E. DePristo, J. Chem. Phys. **93**, 1556 (1989).

[13] M. E. Garcia, G. M. Pastor, and K. H. Bennemann, Phys. Rev. Lett. **67**, 1142 (1991).

[14] P. Delaly, P. Ballone, and J. Buttet, Phys. Rev. B **45**, 3838 (1992).

[15]G. S. Painter, Phys. Rev. Lett. **70**, 3959 (1993).
[16]L. J. Sham, Phys. Rev. B **32**, 3876 (1985), and references therein.
[17]R. G. Parr and W. Yang, *Density-Functional Theory of Atoms and Molecules* (Oxford University Press, New York, 1989).
[18]S. H. Vosko, L. Wilk, and M. Nusair, Can. J. Phys. **58**, 1200 (1980); G. S. Painter, Phys. Rev. B **24**, 4284 (1981).
[19]G. S. Painter and F. W. Averill, Phys. Rev. B **28**, 5536 (1983).
[20]A. J. H. Wachters, J. Chem. Phys. **52**, 1033 (1970).
[21]P. J. Hay, J. Chem. Phys. **66**, 4377 (1977).
[22]F. B. van Duijneveldt, IBM Research Report No. RJ-945, 1971.
[23]C. Kittel, *Introduction to Solid State Physics* (Wiley, New York, 1971).
[24]The same energy difference across a series is observed in results from the rectangular band model (see Ref. 25), with nearest-neighbor hopping, in application to the 4*d* transition-metal series. The energy difference between theory and experiment there is also about 2.0 eV/atom.
[25]D. G. Pettifor, in *Solid State Physics* (Ref. 3), Vol. 40, p. 74.
[26]Results for the crystal are from LDA energy-band calculations of Ref. 27 and are non-spin-polarized *except* for Fe, Ni, and Co (both cohesive energy and lattice spacing calculated including spin polarization) and Cr and Mn (only lattice spacing calculated including spin polarization).
[27]V. L. Morruzi, J. F. Janak and A. R. Williams, *Calculated Electronic Properties of Metals* (Pergamon, New York, 1978).
[28]The weakness of the Mn_2 bond is further accentuated in non-spin-polarized calculations where the binding is even less (0.1 eV/atom).
[29]The Be_6 cluster binding energy (and bond length) is in good agreement with the LDA model potential results given in Ref. 30.
[30]E. Blaisten-Barojas and S. N. Khanna, Phys. Rev. Lett. **61**, 1477 (1988).
[31]W. H. Press, B. P. Flannery, S. H. Teukolsky, and W. T. Vetterling, *Numerical Recipes* (Cambridge University Press, New York, 1986), p. 484.
[32]J. F. Janak and A. R. Williams, Phys. Rev. B **14**, 4199 (1976).
[33]B. K. Rao and P. Jena, Phys. Rev. B **32**, 2058 (1985).
[34]F. Reuse, S. N. Khanna, V. deCoulon, and J. Buttet, Phys. Rev. B **41**, 11 743 (1990).
[35]K. P. Huber and G. L. Herzberg, *Molecular Spectra and Molecular Structure. IV Constants of Diatomic Molecules* (Van Nostrand Reinhold, New York, 1979).
[36]A. R. Williams, C. D. Gelatt Jr., and J. F. Janak, in *Theory of Alloy Phase Formation,* edited by L. H. Bennett (The Metallurgical Society of AIME, New Orleans, 1979), p. 40.
[37]A. R. Williams and U. von Barth, in *Theory of the Inhomogeneous Electron Gas,* edited by S. Lundqvist and N. H. March (Plenum, New York, 1983), p. 189.
[38]D. G. Pettifor, in *Physical Metallurgy, Part I,* edited by R. W. Cahn and P. Haasen (Elsevier, Amsterdam, 1983), p. 127.
[39]J. H. Rose and H. B. Shore, Phys. Rev. B **43**, 11 605 (1991).
[40]Y. Jinlong, W. Kelin, F. Casula, and G. Mula, Phys. Rev. B **47**, 4025 (1993).
[41]S. N. Khanna and P. Jena, Phys. Rev. Lett. **69**, 1664 (1992).